



Dickie, E. A., Young, S. A. and Smith, T. K. (2019) Substrate specificity of the neutral sphingomyelinase from *Trypanosoma brucei*. *Parasitology*, 146(5), pp. 604-616. (doi:[10.1017/S0031182018001853](https://doi.org/10.1017/S0031182018001853))

There may be differences between this version and the published version. You are advised to consult the publisher's version if you wish to cite from it.

<http://eprints.gla.ac.uk/197303/>

Deposited on: 21 November 2018

Enlighten – Research publications by members of the University of Glasgow
<http://eprints.gla.ac.uk>

1

2

Full title: Investigating the Substrate Specificity of the Neutral Sphingomyelinase

3

from *Trypanosoma brucei*

4

5

Emily A. Dickie¹, Simon A. Young and Terry K. Smith

6

7

Biomedical Sciences Research Complex, Schools of Biology and Chemistry,

8

University of St Andrews, Fife, KY16 9ST, UK

9

10

Running title: *T. brucei* neutral sphingomyelinase substrate specificity

11

12

Correspondence should be addressed to Terry K. Smith. Address: Biomedical Sciences

13

Research Complex, Schools of Biology and Chemistry, University of St Andrews, Fife,

14

KY16 9ST, UK. Telephone: +44(0)1334 463412. Email: tks1@st-andrews.ac.uk

15

¹ Current address: Wellcome Trust Centre for Molecular Parasitology, Institute of Infection, Immunity and Inflammation, College of Medical, Veterinary and Life Sciences, University of Glasgow, Glasgow, G12 8TA, UK

16 **ABSTRACT**

17 The kinetoplastid parasite *Trypanosoma brucei* causes African trypanosomiasis in both
18 humans and animals. Infections place a significant health and economic burden on
19 developing nations in sub-Saharan Africa, but few effective anti-parasitic treatments are
20 currently available. Hence, there is an urgent need to identify new leads for drug
21 development. The *T. brucei* neutral sphingomyelinase (TbnSMase) was previously
22 established as essential to parasite survival, consequently being identified as a potential drug
23 target. This enzyme may catalyse the single route to sphingolipid catabolism outside the
24 *T. brucei* lysosome. To obtain new insight into parasite sphingolipid catabolism, the substrate
25 specificity of TbnSMase was investigated using electrospray ionization tandem mass
26 spectrometry (ESI-MS/MS). TbnSMase was shown to degrade sphingomyelin,
27 inositol-phosphoceramide and ethanolamine-phosphoceramide sphingolipid substrates,
28 consistent with the sphingolipid complement of the parasites. TbnSMase also catabolised
29 ceramide-1-phosphate, but was inactive towards sphingosine-1-phosphate. The broad-range
30 specificity of this enzyme towards sphingolipid species is a unique feature of TbnSMase.
31 Additionally, ESI-MS/MS analysis revealed previously uncharacterised activity towards
32 *lyso*-phosphatidylcholine (*lyso*-PC), despite the enzyme's inability to degrade PC.
33 Collectively, these data underline the enzyme's importance in choline homeostasis and the
34 turnover of sphingolipids in *T. brucei*.

35 **KEYWORDS:** lipid catabolism, sphingolipid, choline, lipid extraction, mass spectrometry,
36 enzyme, activity assay

37

38 KEY FINDINGS

- 39 • TbnSMase has broad substrate specificity towards various sphingolipids
- 40 • TbnSMase is the first *T. brucei* enzyme shown to catabolise *lyso*-phosphatidylcholine
- 41 • Sphingosine-1-phosphate, glycosphingolipids and phosphatidylcholine are not
- 42 TbnSMase substrates
- 43 • TbnSMase plays a direct role in choline homeostasis in bloodstream form parasites

44 INTRODUCTION

45 The kinetoplastid parasite *Trypanosoma brucei* causes African trypanosomiasis in both
46 humans and animals. Human African trypanosomiasis (HAT) is considered fatal if left
47 untreated, and poses a serious health risk to an estimated 65 million people in Sub-Saharan
48 Africa (World Health Organization, 2017a). Recent efforts have led to a dramatic decrease in
49 reported disease cases, with 2804 cases reported in 2015, although the World Health
50 Organization estimates the actual number of cases to be 10-fold greater (World Health
51 Organization, 2017a; b). Research has also produced promising new drug candidates,
52 however, the risk of parasite resistance and consequent HAT re-emergence still threaten the
53 progress made in combatting the disease. Animal trypanosomiasis remains a significant
54 burden, with billions of US dollars lost through livestock infections each year and few
55 treatment candidates on the horizon (Shaw *et al.*, 2014). Thus, there is an urgent need to
56 identify leads for drug development.

57 *T. brucei* sphingolipid biosynthesis has long been identified as a potential drug target. Most
58 eukaryotes are capable of synthesising their own sphingolipids via the *de novo* biosynthesis
59 pathway (**Fig. 1A**), which is highly conserved amongst eukaryotic organisms (Kolter and
60 Sandhoff, 1999). Although homologues of most of the enzymes involved in this biosynthetic
61 pathway have been (putatively) identified in *T. brucei*, many still require biochemical
62 characterisation (Smith and Bütikofer, 2010). The first reaction in the pathway, condensation
63 of serine and palmitoyl-CoA, is catalysed by the enzyme serine-palmitoyltransferase (SPT)
64 (Tidhar and Futerman, 2013). A homologue of this enzyme has been identified in *T. brucei*,
65 which was shown to be essential for cell cycle progression and parasite survival (Fridberg *et al.*
66 *et al.*, 2008). Inhibiting the initial SPT-catalysed reaction of the *T. brucei de novo* biosynthesis
67 pathway disrupted procyclic cytokinesis and kinetoplast segregation, validating the pathway
68 as a drug target (Fridberg *et al.*, 2008; Smith and Bütikofer, 2010). Although SPT is known to

69 be essential in other parasites, such as *Plasmodium falciparum* (Gerold and Schwarz, 2001),
70 these findings contrast with research involving the related kinetoplastid parasite *Leishmania*
71 *major* (Denny *et al.*, 2004; Zhang *et al.*, 2007). Unusually, *T. brucei* has four tandemly linked
72 genes, each encoding different sphingolipid synthases (TbSLSs1-4) (Sevova *et al.*, 2010).
73 This family of sphingolipid synthases is orthologous to the *S. cerevisiae* *AURI*-encoded IPC
74 synthase (Mina *et al.*, 2009), and equivalent enzymes are found in both *Leishmania major*
75 (Denny *et al.*, 2006) and *Trypanosoma cruzi* (De Lederkremer *et al.*, 2011). RNA
76 interference (RNAi) against the *TbSLS1-4* gene locus in bloodstream trypanosomes impeded
77 growth, ultimately leading to parasite death (Sutterwala *et al.*, 2008). This finding identified
78 the TbSLSs as potential drug targets. The individual functional specificities of the four
79 synthases were determined by employing a cell-free synthesis system (Sevova *et al.*, 2010).
80 TbSLSs 1 and 2 synthesise IPC and EPC respectively (Sevova *et al.*, 2010). TbSLSs 3 and 4
81 are bi-functional, producing both SM and EPC (Sevova *et al.*, 2010). Research has indicated
82 TbSLS substrate specificity is dictated by natural variations in a small number of active site
83 residues, thought to be involved in acid-base catalysis (Goren *et al.*, 2011). Establishing the
84 functions of the TbSLSs has clarified how the parasite is capable of altering its sphingolipid
85 complement during its life cycle (Mina *et al.*, 2009; Sevova *et al.*, 2010), an observation
86 further confirmed by recent sphingolipidomic analysis (Guan and Mäser, 2017). Currently,
87 trypanosomatids are the only organisms known to synthesise sphingolipid species with
88 choline, ethanolamine and inositol headgroups (Serricchio and Bütikofer, 2011; Guan and
89 Mäser, 2017).

90 In comparison to the knowledge of *T. brucei* sphingolipid biosynthesis that has already been
91 acquired, little is known of the processes involved in the parasites' sphingolipid catabolism.
92 The catabolism of sphingolipids in eukaryotes takes place via the degradation pathway
93 (**Fig. 1B**), predominantly in lysosomes and late endosomes, but also in other cellular
94 locations (Kolter and Sandhoff, 1999; Jenkins *et al.*, 2009). A number of different enzymes
95 are involved in the degradative process (ceramidases, lyases, phospholipase D), but one
96 major group of proteins responsible for sphingolipid turnover in mammalian cells is the
97 sphingomyelinase (SMase) enzyme family (Kolter and Sandhoff, 1999). As indicated by their
98 name, the primary substrate of these enzymes in mammals is SM, which is hydrolysed to
99 yield ceramide and choline-phosphate (ChoP) (Jenkins *et al.*, 2011). *T. brucei* has a single
100 neutral SMase (TbnSMase) (Q57U95), a membrane protein with two identified
101 transmembrane domains at its C-terminus (Young and Smith, 2010). TbnSMase has been

102 localised to the ER in bloodstream form parasites, and genetically confirmed as a potential
103 drug target (Young and Smith, 2010). The activity of this protein is thought to be essential
104 due to its intrinsic roles in vital biochemical processes, including choline and ceramide
105 homeostasis, and endocytosis. This is particularly relevant to the coupling of endocytic and
106 exocytic mechanisms with post-Golgi sorting of GPI-anchored variant surface glycoprotein
107 (VSG), which is needed to maintain VSG surface density (Young and Smith, 2010). VSG
108 molecules form the protective coat that permits *T. brucei* parasites to evade the host immune
109 system (Mugnier *et al.*, 2016). The importance of TbnSMase corroborates findings relating to
110 the single leishmanial sphingolipid degradative enzyme (ISCL), another nSMase homologue
111 (Zhang *et al.*, 2009; McConville and Naderer, 2011). ISCL IPCase activity is required for
112 *L. major* promastigote stationary phase survival, most noticeably at acidic pH (Xu *et al.*,
113 2011). The enzyme's SMase function is necessary for amastigote proliferation and virulence
114 in mammalian hosts (Zhang *et al.*, 2009, 2012). This means that the importance of
115 leishmanial ISCL activity is linked to cell cycle stage (Zhang *et al.*, 2012). Similarly,
116 inhibiting the nSMase/*lyso*-PC phospholipase C of *Plasmodium falciparum* disrupts parasite
117 intra-erythrocytic proliferation, suggesting the protein could serve as a drug target (Hanada *et*
118 *al.*, 2002). In previous research, TbnSMase was shown to catabolise SM effectively, but was
119 inactive towards phosphatidylcholine (PC) (Young and Smith, 2010). This initial analysis has
120 now been taken forward to provide a more comprehensive overview of TbnSMase lipid
121 degradative activity and specificity.

122 MATERIALS AND METHODS

123 Unless otherwise stated, all reagents and materials were purchased from Sigma, Promega,
124 Thermo Scientific or VWR. C-1-P (d18:1/16:0), EPC (d17:1/12:0), SM (brain, porcine),
125 dipalmitoyl-PC and dimyristoyl-PC (used as a mass spectrometry standard) were purchased
126 from Avanti Polar Lipids. SM (D18:1/6:0), *lyso*-PC (from egg yolk), S-1-P (d18:1), and
127 galactosylceramide were purchased from Sigma. EPC (from buttermilk, semi-synthetic) was
128 purchased from Matreya LLC. Procytic cell culture media were filter sterilised with either
129 Millex GP 0.22 μ M syringe filters or Triple Red 0.22 μ M vacuum filtration units. Parasite
130 cultures were maintained in Greiner Bio-One CELLSTAR® tissue culture flasks.

131

132

133 Recombinant expression of TbnSMase (Q57U95) in *E. coli*

134 A pGEX-6P-1-TbnSMase expression construct was employed as previously described
135 (Young and Smith, 2010). The expression construct was used to transform BL21 pLysSGold
136 *E. coli*. Positive clones were selected using ampicillin-agar plates ($100 \mu\text{g mL}^{-1}$)
137 supplemented with chloramphenicol ($34 \mu\text{g mL}^{-1}$). Three bacterial colonies were used to
138 inoculate 3×10 mL of LB media (Miller composition, supplemented with $50 \mu\text{g mL}^{-1}$
139 ampicillin and $34 \mu\text{g mL}^{-1}$ chloramphenicol). After a 24 hour incubation, the 10 mL
140 overnight cultures were combined in a single tube (30 mL total volume). The combined
141 culture was then used to inoculate 3×1 L auto-induction (AI) media (Formedium,
142 supplemented with $50 \mu\text{g mL}^{-1}$ ampicillin and $34 \mu\text{g mL}^{-1}$ chloramphenicol), using 10 mL of
143 overnight culture per litre flask of AI media. Cells were grown at 37°C for 4 hours before the
144 temperature was decreased to 25°C for a further 20 -hour incubation.
145 GST-TbnSMase-enriched bacterial membranes were prepared from these cultures. Pellets of
146 500 mL spun-down culture were washed in PBS and stored at -80°C until they could be
147 processed.

148 TbnSMase-enriched bacterial membrane preparation

149 The protocol described is adapted from methods previously outlined (Young and Smith,
150 2010). Pellets of 500 ml spun-down bacterial culture were suspended and lysed in 10 mL
151 lysis buffer (50 mM Tris.HCl (pH 8.0), 300 mM NaCl, 10% glycerol (v/v), 5 mM MgCl_2 ,
152 1 mM DTT), containing 0.2 mg mL^{-1} lysozyme (Sigma), Merck Millipore Benzonase®
153 Endonuclease ($250 \text{ units mL}^{-1}$ lysate) and 1 x protease inhibitor tablet (Roche). The lysis
154 solution was incubated for 30 minutes at 37°C , followed by probe sonication at 4°C
155 (6 minutes total, 30 seconds on/30 seconds off). The lysate was then centrifuged at
156 $14,500 \times g$, 20 minutes. The product supernatant was divided amongst 3.2 mL capacity
157 Beckman Coulter ultra-centrifuge tubes (x 3) for ultra-centrifugation at $100,000 \times g$, 1 hour.
158 Pellets were washed with 1.5 mL PBS. Bacterial membrane pellets were then suspended in
159 $500 \mu\text{L}$ buffer each (100 mM Tris-HCl (pH 7.4), 10 mM MgCl_2 , 20% glycerol) using a
160 combination of vortexing and water bath sonication (25°C , 4 minutes). The total membrane
161 suspension ($1500 \mu\text{L}$ total volume) was mixed in a single tube and was then aliquoted
162 ($50\text{-}100 \mu\text{L}$). Aliquots were flash-frozen using liquid nitrogen and stored at -80°C . Total
163 protein in each membrane preparation was quantified using the BCA Protein Assay Kit

164 (Thermo Scientific). The presence of TbnSMase in bacterial membranes was confirmed by
165 mass spectrometry.

166 Amplex® UltraRed assay

167 Amplex® UltraRed assay coupling enzyme solutions were prepared from lyophilized
168 powders using dH₂O, and were stored as small aliquots at -20°C. Alkaline phosphatase
169 (AlkPhos) (Sigma) from bovine intestinal mucosa was prepared as a 400 units mL⁻¹ stock
170 solution. Choline oxidase (ChoOx) (Sigma) from *Alcaligenes* sp. was prepared at
171 20 units mL⁻¹, horseradish peroxidase (HRP) (Sigma) at 200 units mL⁻¹. Desiccated aliquots
172 of Amplex® UltraRed reagent (Thermo Scientific) were suspended in 340 µL DMSO, as
173 directed by the manufacturer, and stored at -20°C in small aliquots. To assay the aqueous
174 fractions of biphasically separated GST-TbnSMase SM substrate reactions, aqueous phases
175 were dried using a Savant SPD121P SpeedVac concentrator. The fractions were suspended in
176 100 µL reaction buffer (100 mM HEPES (pH 7.4), 10 mM MgCl₂) and divided between
177 2 wells of a black 96-well reaction plate (50 µL per well). Additional reaction buffer (50 µL)
178 was then added to each well. A mastermix of Amplex® assay components (coupling enzymes
179 and Amplex® UltraRed reagent) was prepared. The mastermix accounted for the addition of
180 2 µL AlkPhos, 1.5 µL ChoOx, 1 µL HRP, 0.25 µL Amplex UltraRed reagent and 95.25 µL
181 reaction buffer per well (total reaction volume per well was 200 µL). Change in fluorescence
182 (Ex. 560 nm, Em. 587 nm) was then monitored for 1 hour using a Spectra Max Gemini XPS
183 fluorescence plate reader at 37°C. Results were recorded using SoftMax Pro v 5.2 software.

184 Lipid substrate activity assays

185 Lipid substrates were suspended in 2% Triton X-100 to the desired stock concentration
186 through vortexing and water-bath sonication (10 minutes). Substrate mass was substrate- and
187 analysis-dependent (20-50 nmoles), but each was added to reactions (50-100 µL total
188 volume) to a final concentration of 0.1-0.2% Triton X-100. Substrates were incubated with
189 TbnSMase-enriched bacterial membranes (~100 µg total protein) in 1.5 mL
190 solvent-resistant microcentrifuge tubes. In heat-inactivated protein reactions, protein aliquots
191 were heated to 95°C (20 minutes) prior to substrate addition. Reactions were performed in
192 100 mM HEPES (pH 7.4), 10 mM MgCl₂ buffer. On substrate addition, reactions were mixed
193 briefly and sonicated for 30 seconds in a water bath (25°C). Reaction tubes were then
194 incubated at 37°C (4 hours) in a water bath. Following incubation, reactions were quenched

195 with 800 μL CHCl_3 . If required, mass spectrometry standards (e.g. PC 28:0) were then added
196 (500 pmoles), prior to the addition of 250 μL dH_2O . The organic phase was isolated
197 following the Bligh and Dyer biphasic separation method (Bligh and Dyer, 1959), and dried
198 under nitrogen.

199 Parasite lysate NBD-IPC activity assays

200 Cells were suspended in lysis buffer (25 mM Tris (pH 7.5), 0.1% Triton X-100, 1 x protease
201 inhibitor tablet (Roche)) to a density of $\geq 2 \times 10^8$ cells mL^{-1} , and were incubated on ice for
202 5 minutes. Subsequently, 4×10^6 parasites from each stock were transferred to each reaction.
203 Parasites were incubated with 0.8 nmoles NBD-IPC, in 50 mM Tris (pH 7.5), 5 mM MgCl_2 ,
204 5 mM DTT, 0.1 % Triton X-100 reaction buffer, for 1 hour at 25 °C with gentle agitation
205 (protected from the light). Following incubation, reactions were quenched with the addition
206 of 1 mL CHCl_3 . Subsequently, 500 μL MeOH and 200 μL dH_2O were quickly added.
207 Samples were vortex mixed, then left to stand (protected from the light). The organic phase
208 from each sample was isolated through biphasic separation, and dried under nitrogen.

209 High-performance thin-layer chromatography

210 HPTLC analysis of EPC and NBD-IPC substrate reactions was conducted using a
211 CHCl_3 : MeOH: dH_2O solvent system (65:25:4). Dried lipid samples were resuspended in 2:1
212 CHCl_3 : MeOH (10-20 μL volume) and were gradually spotted onto HPTLC plates.
213 EPC reaction results were visualised by treating HPTLC plates with ninhydrin solution
214 (1% w/v in butan-1-ol). NBD-IPC reaction results were visualised via fluorescence imaging
215 using a Typhoon FLA 7000 (GE), with CY2 (filter Y520, 473 nm laser) and Sypro Ruby
216 (filter O580, 473 nm laser) settings.

217 Procyclic form *T. brucei* lipid extract preparation

218 *T. brucei* (Lister 427 (29-13) strain) procyclic (PCF) parasites were grown in SDM-79 media
219 at pH 7.4, as previously described (Brun and Schönenberger, 1979). Drugs G418
220 ($15 \mu\text{g mL}^{-1}$) and hygromycin ($50 \mu\text{g mL}^{-1}$) were included in the media in order to maintain
221 the expression of a tetracycline repressor and T7 RNA polymerase (Wirtz *et al.*, 1999). A
222 10 ml culture of PCF cells ($\sim 1 \times 10^7$ cells mL^{-1}) was pelleted via centrifugation at 800 x g,
223 10 minutes. The cell pellet was resuspended in a minimal volume of media ($\sim 500 \mu\text{L}$) and
224 transferred to a microcentrifuge tube for further centrifugation (3800 x g, 3 minutes). Cells

225 were washed in 1 mL PBS, and then re-pelleted (3800 x g, 3 minutes). The pellet was
226 resuspended in 200 μ L PBS and transferred to a glass vial containing 750 μ L 2:1
227 MeOH:CHCl₃ for biphasic separation, based on the method described by Bligh and Dyer
228 (Bligh and Dyer, 1959). The sample was dried under nitrogen and stored at 4°C until use.

229 Electrospray tandem mass spectrometry

230 Lipid samples were analysed by electrospray tandem mass spectrometry (ESI-MS/MS) with
231 an AB-Sciex Qtrap 4000 triple quadrupole mass spectrometer, incorporating an Advion
232 TriVersa NanoMate nanoelectrospray ionisation source. Single-stage MS in negative ion
233 mode was used to obtain survey scans of phosphatidylethanolamine (PE),
234 ethanolamine-phosphoceramide (EPC), phosphatidylinositol (PI), inositol-phosphoceramide
235 (IPC) and ceramide (Cer) species (cone voltage = 1.25 kV). Positive ion mode survey scans
236 were used to detect phosphatidylcholine (PC) and sphingomyelin (SM) species
237 (cone voltage = 1.25 kV). In tandem mass spectrometry, nitrogen was the collision gas. To
238 examine PC/SM species, positive ion mode scans to detect precursors of m/z 184 were
239 performed, with 50 eV collision energy (CE). In negative ion mode, precursors of m/z 196
240 scans allowed the identification of PE and EPC lipids, precursors of m/z 241 scans were used
241 to observe PI and IPC species (CE = 60). Spectra were acquired over or within the range of
242 120-1000 m/z, and each spectrum represents a minimum of 30 consecutive scans. Samples
243 were run using a 1:1 solvent mixture of 2:1 MeOH: CHCl₃ and
244 6:7:2 acetonitrile: isopropanol: dH₂O.

245 **RESULTS**

246 GST-TbnSMase was recombinantly expressed in *E. coli* to produce TbnSMase-enriched
247 bacterial membranes, using previously described methods (Young and Smith, 2010). The
248 presence of the GST-TbnSMase membrane protein was confirmed using mass spectrometry
249 (**Fig. S1**). After isolating the bacterial membranes via ultra-centrifugation, it was possible to
250 assay GST-TbnSMase activity directly from the membranes with minimal bacteria-derived
251 background activity, removing the need for protein purification. This had also been achieved
252 during previous research into TbnSMase activity (Young and Smith, 2010). To confirm the
253 GST-TbnSMase recombinant protein was active, GST-TbnSMase-enriched bacterial
254 membranes were first incubated at 37 °C for 4 hours with a sphingomyelin (SM) substrate.
255 The substrate used was Avanti Polar Lipids brain SM (product no. 860062). Although this

256 product is enriched for SM 36:1 (d18:1/18:0), as a natural lipid preparation the product is a
257 mixture of brain SM species. The spectra presented here are consistent with the recently
258 released Avanti Polar Lipids fatty acid distribution analysis for this product (**Fig. S2**)
259 (Avanti Polar Lipids, 2018). Following SM substrate incubation, reactions were biphasically
260 separated using 2:1 CHCl₃: MeOH to isolate the lipid-rich organic phase. ESI-MS/MS was
261 used to detect the levels of choline-containing (SM) lipid species in lipid samples derived
262 from both active GST-TbnSMase and heat-inactivated GST-TbnSMase reactions (**Fig. 2A**
263 **and 2B**, see also **Fig. S3**). A dimyristoyl-PC standard was added to each sample during lipid
264 extraction, allowing SM substrate peak intensities to be normalised against the intensity of
265 the internal standard. Relative peak intensities for each SM substrate species are shown
266 (**Fig. 2C**).

267 The catabolic activity of GST-TbnSMase towards sphingomyelin had been demonstrated
268 previously (Young and Smith, 2010), here providing confirmation that the GST-TbnSMase
269 recombinant protein was active. However, the use of ESI-MS/MS allowed the relative
270 turnover of individual SM species present in the substrate mixture to be compared (**Fig. 2C**).
271 The results indicate that GST-TbnSMase is active towards SM species with a range of
272 fatty acid chain lengths (C16-C24). There was a 2.6-fold (62%) decrease in
273 SM 42:1 (d18:1/24:0)/SM 42:2 (d18:1/24:1), compared to a 1.5-fold (35%) decrease in
274 SM 36:1 (d18:1/18:0), despite the latter lipid being the prevalent species in the SM substrate
275 mixture. This may indicate GST-TbnSMase preferentially degrades sphingolipid species of
276 specific fatty acid chain lengths. SM substrate catabolism was further confirmed by
277 identification of product ceramide chloride adducts [M + Cl]⁻ in negative ion mode survey
278 scans (**Fig. 3**). Product ceramides were observed in the active GST-TbnSMase reaction
279 (**Fig. 3A**), and were absent from the heat-inactivated control (**Fig. 3B**). Additionally, aqueous
280 fractions isolated during biphasic separation of SM substrate reactions were tested for the
281 presence of choline phosphate. The aqueous fractions were used as substrates for the
282 Amplex® UltraRed assay system. In this assay (**Fig. S4**), the coupling enzyme alkaline
283 phosphatase (AlkPhos) is included to dephosphorylate choline phosphate, yielding choline.
284 The choline produced then serves as a substrate for the second coupling enzyme in the
285 system: choline oxidase (ChoOx). Only the aqueous fractions from the active
286 GST-TbnSMase reactions, in the presence of alkaline phosphatase, induced significantly
287 increased rates of fluorescence change (**Fig. 3C**). These results confirm GST-TbnSMase is a

288 phosphodiesterase C enzyme, degrading SM substrates to form ceramide and choline
289 phosphate.

290

291 Having established the GST-TbnSMase protein was active, the enzyme's activity towards a
292 number of different sphingolipid substrates was examined. As already highlighted,
293 *T. brucei* is known to produce SM, EPC and IPC. Thus, it was important to examine the
294 activity of TbnSMase towards EPC and IPC sphingolipids. Firstly, GST-TbnSMase was
295 incubated with an EPC substrate. The EPC substrate used was supplied by Mattreya LLC
296 (product no. 1327), a semi-synthetic preparation derived from bovine buttermilk. No fatty
297 acid distribution analysis is available for this product. However, the average molecular
298 weight reported for the product (mw = 773) appears consistent with our analysis (**Fig. 4A**).
299 Lipid extracts from the EPC substrate reactions were analysed in ESI-MS/MS negative ion
300 mode survey scans. The EPC species present in the substrate (**Fig. 4A**) were efficiently
301 degraded by GST-TbnSMase, yielding ceramide products (**Fig. 4B**). These products were
302 absent from the heat-inactivated GST-TbnSMase control and the EPC/Triton X-100 detergent
303 mixed micelles supplied to the reactions (**Fig. 4C and 4D**). Additionally, GST-TbnSMase
304 degradative activity towards EPC was shown via HPTLC (**Fig. S5**). GST-TbnSMase was also
305 incubated with a lipid substrate mixture containing equimolar concentrations of SM
306 (d18:1/6:0, Avanti Polar Lipids product no.860582) and EPC (d17:1/12:0, Avanti Polar
307 Lipids product no.860529). This competition assay indicated GST-TbnSMase lacks a
308 sphingolipid substrate preference (**Fig. S6**). However, given the high levels of substrate
309 turnover for both species, it is possible increasing the concentrations of both substrates may
310 lead to a more marked preference for SM over EPC. Additionally, as EPC (d17:1/12:0) is the
311 only pure EPC substrate commercially available, it is not possible to assess the impact of
312 varying the sphingoid base and fatty acid composition on substrate turnover.

313

314 Currently, pure IPC lipid species are only available commercially through custom synthesis.
315 GST-TbnSMase was shown to catabolise a custom synthesised NBD-conjugated IPC
316 substrate (**Fig. S7**). However, the synthetic nature of this IPC substrate makes it difficult to
317 draw conclusions regarding the physiological relevance of this activity. It is well established
318 that the prevalent sphingolipid in procyclic form *T. brucei* is IPC (Richmond *et al.*, 2010).
319 Therefore, a lipid extract from procyclic parasites was used to form a mixed micelle IPC
320 substrate for GST-TbnSMase. Negative ion mode scans to detect inositol-containing lipids
321 (precursors of m/z 241) were used to identify the IPC species present in the procyclic

322 *T. brucei* extract (**Fig. 5A**). Negative ion mode survey scans were then employed to search
323 for ceramide chloride adducts [M + Cl]. Significant peaks corresponding to ceramide species
324 were observed in the active GST-TbnSMase reaction (**Fig. 5B**), and were only observed at
325 low levels in the heat-inactivated control (**Fig. 5C, see also Fig. S8**). Taken together, these
326 results suggest GST-TbnSMase is also capable of catabolising natural IPC species to form
327 ceramide and inositol-1-phosphate.

328

329 The ability of GST-TbnSMase to degrade SM, EPC and IPC indicates the enzyme does not
330 distinguish between its sphingolipid substrates based upon headgroup identity. To further
331 explore this finding, GST-TbnSMase was incubated with a ceramide-1-phosphate
332 (d18:1/16:0) substrate (Avanti Polar Lipids product no. 860533). A ceramide (d18:1/16:0)
333 chloride adduct [M + Cl] was apparent in the lipid extract from the active GST-TbnSMase
334 reaction (**Fig. 6A**), and was absent from the control (**Fig. 6B**). This result suggests lipid
335 headgroups are not involved in GST-TbnSMase substrate recognition. However,
336 GST-TbnSMase does not appear to degrade glycosphingolipids, as no apparent catabolism
337 was observed upon incubating GST-TbnSMase with a mixture of galactosylceramide
338 substrate species (Sigma product no. C4905) (data not shown). This indicates that although
339 GST-TbnSMase does not require a headgroup for lipid substrate turnover, features of the
340 headgroup can impede substrate catabolism. It was also observed that the enzyme cannot
341 degrade S-1-P (d18:1, Avanti Polar Lipids product no. 860492), as the level of the substrate
342 species remained unchanged in lipid extracts from an active GST-TbnSMase reaction and
343 controls (data not shown). This finding indicates ceramide is a crucial component of
344 GST-TbnSMase sphingolipid substrates.

345

346 Finally, GST-TbnSMase activity towards choline-containing phospholipids was reassessed.
347 During previous research into TbnSMase, catabolic activity towards PC and *lyso*-PC lipid
348 substrates could not be detected (Young and Smith, 2010). Re-assessing GST-TbnSMase
349 activity towards PC (16:0/16:0) using ESI-MS/MS analysis failed to establish any substrate
350 turnover (Avanti Polar Lipids product no. 850355) (data not shown). However, precursors of
351 m/z 184 scans in positive ion mode revealed that GST-TbnSMase does turnover *lyso*-PC
352 species (**Fig. 7**). There was a marked reduction in *lyso*-PCs (16:0) and (18:0) only in the
353 presence of active GST-TbnSMase (**Fig. 7A**), relative to a PC (10:0/10:0) standard included
354 in all *lyso*-PC reactions. This decrease did not occur in the control (**Fig. 7B**). Additionally,

355 the *lyso*-PC analogues miltefosine and edelfosine were previously shown to inhibit
356 GST-TbnSMase (Young and Smith, 2010). This led to speculation that the previously
357 observed inhibition of the enzyme's activity by *lyso*-PC analogues may be due to these
358 compounds acting as competing substrates. Testing miltefosine as a potential substrate for
359 GST-TbnSMase (5-50 nmoles) in the Amplex® UltraRed assay system did not produce any
360 data to suggest this *lyso*-PC analogue is turned over by GST-TbnSMase (data not shown).
361 This indicates *lyso*-PC analogues are not competitive substrates for GST-TbnSMase.
362 However, the possibility remains that these compounds may be tightly bound to the enzyme's
363 active site, preventing the ChoP release required for assay detection.

364 **DISCUSSION**

365 Sphingolipid metabolism in kinetoplastid parasites has long been established as a potential
366 target for anti-parasitic drug development (Smith and Bütikofer, 2010; Mina and Denny,
367 2017). However, research has focused almost exclusively on the pathways involved in
368 sphingolipid biosynthesis. Initial research into the nSMase found in *T. brucei* showed this
369 enzyme has sphingolipid catabolic activity (Young and Smith, 2010). TbnSMase is the only
370 currently identified *T. brucei* protein that displays this function. Unusually, the parasites
371 appear to lack phospholipase D activity, which generally facilitates eukaryotic SM and PC
372 catabolism. The substrate specificity of TbnSMase was examined to improve understanding
373 of *T. brucei* sphingolipid catabolism and salvage.

374
375 TbnSMase is now known to turnover SM, EPC and IPC sphingolipid species. This is
376 consistent with the established sphingolipid composition of *T. brucei* (Richmond *et al.*, 2010;
377 Guan and Mäser, 2017): IPC predominates in procyclic parasites, whilst almost equal
378 proportions of SM and EPC species are found in the bloodstream form
379 (Guan and Mäser, 2017). In light of this knowledge, it may seem unsurprising that TbnSMase
380 is active towards all three of these sphingolipid classes, only distinguished structurally by
381 their headgroup (choline, ethanolamine and inositol). However, to our knowledge, this
382 breadth of sphingolipid substrate specificity has not been documented previously for a lipid
383 catabolic enzyme. It is possible that other sphingolipid degradative enzymes (especially those
384 found in other kinetoplastids) share this ability but have not been tested. If this wide-ranging
385 substrate specificity is not found in mammalian nSMase homologues, it may be possible to
386 exploit these differences to create TbnSMase-specific substrate analogue inhibitors. The

387 TbnSMase activity reported here precludes the need for other sphingolipid degradative
388 enzymes in the ER and rationalises the constitutive expression of this enzyme in both
389 procyclic and bloodstream forms. However, no activity towards glycosphingolipids was
390 observed, indicating phosphate groups may be an obligatory feature of TbnSMase substrates.
391 It has been reported that *T. brucei* possess trace levels of glycosphingolipids,
392 glucosylceramide species having been identified in several studies (Uemura *et al.*, 2006;
393 Fridberg *et al.*, 2008; Richmond *et al.*, 2010). These could be endocytosed host
394 glycosphingolipids, as no glycosphingolipid biosynthetic enzymes have been formally
395 identified in *T. brucei* (Uemura *et al.*, 2006; Richmond *et al.*, 2010; Guan and Mäser, 2017).
396 Only galactosylceramide species were tested as possible substrates for TbnSMase, thus it
397 remains possible the enzyme is active towards other glycosphingolipids. Alternatively,
398 another (other) unidentified enzyme(s) may be responsible for *T. brucei* glycosphingolipid
399 catabolism, possibly within the lysosome.

400

401 ESI-MS/MS analysis indicates that TbnSMase preferentially catabolises SM species with
402 specific fatty acid chain lengths. A more significant decrease in SM 42:1 (d18:1/24:0)/
403 SM 42:2 (d18:1/24:1) occurred relative to SM 36:1 (d18:1/18:0), despite the latter species
404 being more prevalent in the substrate mixture. This suggests that TbnSMase activity may be
405 geared towards recycling specific long-chain fatty acids, which can then be utilised in other
406 biosynthetic processes. Defining a crystal structure for TbnSMase may reinforce these
407 preliminary observations, particularly if the structure provides insight into substrate binding
408 and potential regulation. Few crystal structures for nSMase proteins are currently available,
409 and most studies have focused on the binding of choline phosphate to the active site
410 (Openshaw *et al.*, 2005; Ago *et al.*, 2006). However, TbnSMase does not seem to distinguish
411 between its substrates based on headgroup identity, instead appearing to preferentially
412 degrade substrates with specific fatty acids. This finding indicates that the fatty acid
413 composition of lipid substrates may be of greater interest when considering enzyme-substrate
414 interactions. In support of this view, TbnSMase was shown to actively degrade
415 ceramide-1-phosphate, which lacks a polar alcohol headgroup entirely. However, the enzyme
416 was unable to catabolise sphingosine-1-phosphate, indicating the presence of an amide bound
417 fatty acid at the *sn*-2 position is vital for sphingolipid substrate recognition. Indeed, in the
418 case of TbnSMase, the critical aspect of lipid substrate recognition appears to centre on the
419 binding of the phosphate and fatty acid moieties to sphingosine or glycerol backbones.

420 TbnSMase is now known to degrade *lyso*-PC in addition to sphingolipids. This aspect of

421 TbnSMase activity brings the enzyme in line with the nSMase found in *Plasmodium*
422 *falciparum* parasites (PfnSMase) (Hanada *et al.*, 2002). Both PfnSMase and TbnSMase are
423 inactive towards PC substrates, despite their ability to degrade *lyso*-PCs. This points to the
424 diacylglycerol moiety of phospholipids impairing substrate binding to these SMase enzymes,
425 and that removal of the fatty acid at the *sn*-2 position alleviates this inhibition. Thus, the
426 requirements for glycerophospholipid recognition are the inverse of sphingophospholipid
427 recognition.

428

429 TbnSMase is the first identified *T. brucei* enzyme shown to be capable of degrading
430 *lyso*-PCs, which are believed to be a primary source of parasite choline during bloodstream
431 infection (Bowes *et al.*, 1993; Smith and Bütikofer, 2010; Macêdo *et al.*, 2013). This is due to
432 the parasites lacking a choline *de novo* biosynthesis pathway (Smith and Bütikofer, 2010),
433 and *lyso*-PC concentration in the blood being 10-fold greater than choline (Macêdo *et al.*,
434 2013). Mammalian bloodstream *T. brucei* require an abundant source of choline, as over 50%
435 of their lipid complement consists of choline-containing lipids (Smith and Bütikofer, 2010).
436 The *T. brucei* phospholipase A₁ was shown to degrade PC, but not *lyso*-PC species
437 (Richmond and Smith, 2007a; b). A plasma membrane phospholipase that degrades *lyso*-PC
438 has been postulated (Bowes *et al.*, 1993) but has yet to be identified. This activity in
439 TbnSMase indicates the enzyme may be responsible for *lyso*-PC turnover in the ER. Research
440 into the essentiality of TbnSMase showed that compromised enzyme function led to a
441 concomitant decrease in the parasite's rate of endocytosis (Young and Smith, 2010). This
442 could have wide-ranging effects on the parasites, but was thought to have particularly
443 impacted *T. brucei* choline homeostasis due to the parasites' dependence upon endocytosed
444 and recycled choline-containing lipids. This impact was indicated by a marked decrease in
445 phosphatidylcholine (PC) and increased intracellular diacylglycerol (DAG), suggesting
446 PC *de novo* biosynthesis via the Kennedy pathway had been disrupted (Young and Smith,
447 2010). The newly discovered ability of TbnSMase to degrade *lyso*-PC and SM species aligns
448 with these observations, indicating decreased enzyme activity has a direct impact on choline
449 homeostasis. This underlines the importance of TbnSMase function in sustaining the
450 intracellular choline metabolite levels required for parasite survival and propagation.

451

452 Further research is required to identify and characterise other enzymes that underpin lipid
453 catabolism and salvage in these kinetoplastid parasites, which represent a valuable model

454 system for eukaryotic lipid metabolism (Serricchio and Bütikofer, 2011). As in the case of
455 TbnSMase, the activity of these enzymes may prove vital, opening new areas of *T. brucei*
456 biochemistry to drug development.

457 **ACKNOWLEDGEMENTS**

458 NBD-inositol-phosphoceramide (NBD-IPC) was kindly gifted by Dr. K. Zhang (Texas Tech
459 University).

460 **FINANCIAL SUPPORT**

461 This work was supported primarily through the European Community's Seventh Framework
462 Programme under grant agreements No. 602773 (Project KINDRED), with additional support
463 from Wellcome Trust Project grant (086658); Medical Research Council (MR/Mo20118/1)
464 and the School of Chemistry (The University of St Andrews).

465

466 REFERENCES

- 467
468 **Ago, H, Oda, M, Takahashi, M, Tsuge, H, Ochi, S, Katunuma, N, Miyano, M and**
469 **Sakurai, J** (2006) Structural basis of the sphingomyelin phosphodiesterase activity in
470 neutral sphingomyelinase from *Bacillus cereus*. *Journal of Biological Chemistry* **281**,
471 16157–67. doi: 10.1074/jbc.M601089200.
- 472 **Avanti Polar Lipids** (2018) 860062 Brain SM, Sphingomyelin (Brain, Porcine). Retrieved
473 from Avanti Polar Lipids website: <https://avantilipids.com/product/860062> (accessed 24
474 January 2018)
- 475 **Bligh, EG, Dyer, WJ** (1959) A Rapid Method of total Lipid Extraction and Purification.
476 *Canadian Journal of Biochemistry and Physiology* **37**, 911–917. doi: 10.1139/o59-099
- 477 **Bowes, E, Samad, H, Jiang, P, Weaver, B and Mellors, A** (1993) The acquisition of
478 lysophosphatidylcholine by African trypanosomes. *Journal of Biological Chemistry* **268**,
479 13885–92.
- 480 **Brun, R and Schönenberger, M** (1979) Cultivation and in vitro cloning or procyclic culture
481 forms of *Trypanosoma brucei* in a semi-defined medium. Short communication. *Acta*
482 *Tropica* **36**, 289–292. doi: 10.5169/seals-312533.
- 483 **De Lederkremer, RM, Agusti, R and Docampo, R** (2011) Inositolphosphoceramide
484 metabolism in *Trypanosoma cruzi* as compared with other trypanosomatids. *Journal of*
485 *Eukaryotic Microbiology* **58**, 79–87. doi: 10.1111/j.1550-7408.2011.00533.x.
- 486 **Denny, PW, Goulding, D, Ferguson, MAJ and Smith, DF** (2004) Sphingolipid-free
487 *Leishmania* are defective in membrane trafficking, differentiation and infectivity.
488 *Molecular Microbiology* **52**, 313–27. doi: 10.1111/j.1365-2958.2003.03975.x.
- 489

- 490 **Denny, PW, Shams-Eldin, H, Price, HP, Smith, DF and Schwartz, RT** (2006) The
491 protozoan inositol phosphorylceramide synthase: a novel drug target which defines a new
492 class of sphingolipid synthase. *Journal of Biological Chemistry* **281**, 28200–28209. doi:
493 10.1074/jbc.M600796200
- 494 **Fridberg, A, Olson, CL, Nakayasu, ES, Tyler, KM, Almeida, IC and Engman, DM**
495 (2008) Sphingolipid synthesis is necessary for kinetoplast segregation and cytokinesis in
496 *Trypanosoma brucei*. *Journal of Cell Science* **121**, 522–35. doi: 10.1242/jcs.016741.
- 497 **Gerold, P and Schwarz, RT** (2001) Biosynthesis of glycosphingolipids de-novo by the
498 human malaria parasite *Plasmodium falciparum*. *Molecular and Biochemical*
499 *Parasitology* **112**, 29–37. doi: 10.1016/S0166-6851(00)00336-4.
- 500 **Goren, MA, Fox, BG and Bangs, JD** (2011) Amino acid determinants of substrate
501 selectivity in the *Trypanosoma brucei* sphingolipid synthase family. *Biochemistry* **50**,
502 8853–8861. doi: 10.1021/bi200981a.
- 503 **Guan, XL and Mäser, P** (2017) Comparative sphingolipidomics of disease-causing
504 trypanosomatids reveal unique lifecycle- and taxonomy-specific lipid chemistries.
505 *Scientific Reports* **7**, 1–13. doi: 10.1038/s41598-017-13931-x.
- 506 **Hanada, K, Palacpac, NMQ, Magistrado, PA, Kurokawa, K, Rai, G, Sakata, D, Hara,**
507 **T, Horii, T, Nishijima, M and Mitamura, T** (2002) *Plasmodium falciparum*
508 phospholipase C hydrolyzing sphingomyelin and lysocholinephospholipids is a possible
509 target for malaria chemotherapy. *Journal of Experimental Medicine* **195**, 23–34.
- 510 **Jenkins, RW, Canals, D and Hannun, YA** (2009) Roles and regulation of secretory and
511 lysosomal acid sphingomyelinase. *Cellular Signalling* **21**, 836–846. doi:
512 10.1016/j.cellsig.2009.01.026.
513

- 514 **Jenkins, RW, Idkowiak-Baldys, J, Simbari, F, Canals, D, Roddy, P, Riner, CD, Clarke,**
515 **CJ and Hannun, YA** (2011) A novel mechanism of lysosomal acid sphingomyelinase
516 maturation: requirement for carboxyl-terminal proteolytic processing. *Journal of*
517 *Biological Chemistry* **286**, 3777–88. doi: 10.1074/jbc.M110.155234.
- 518 **Kolter, T and Sandhoff, K** (1999) Sphingolipids-Their Metabolic Pathways and the
519 Pathobiochemistry of Neurodegenerative Diseases. *Angewandte Chemie (International*
520 *ed. in English)* **38**, 1532–1568. doi: 10.1002/(SICI)1521-
521 3773(19990601)38:11<1532::AID-ANIE1532>3.0.CO;2-U
- 522 **Macêdo, JP, Schmidt, RS, Mäser, P, Rentsch, D, Vial, HJ, Sigel, E and Bütikofer, P**
523 (2013) Characterization of choline uptake in *Trypanosoma brucei* procyclic and
524 bloodstream forms. *Molecular and Biochemical Parasitology* **190**, 16–22. doi:
525 10.1016/j.molbiopara.2013.05.007.
- 526 **McConville, MJ and Naderer, T** (2011) Metabolic pathways required for the intracellular
527 survival of *Leishmania*. *Annual Review of Microbiology* **65**, 543–61. doi:
528 10.1146/annurev-micro-090110-102913.
- 529 **Mina, JGM and Denny, PW** (2017) Everybody needs sphingolipids, right! Mining for new
530 drug targets in protozoan sphingolipid biosynthesis. *Parasitology* 1–14. doi:
531 10.1017/S0031182017001081.
- 532 **Mina, JG, Pan, S-Y, Wansadhipathi, NK, Bruce, CR, Shams-Eldin, H, Schwarz, RT,**
533 **Steel, PG and Denny, PW** (2009) The *Trypanosoma brucei* sphingolipid synthase, an
534 essential enzyme and drug target. *Molecular and Biochemical Parasitology* **168**, 16–23.
535 doi: 10.1016/j.molbiopara.2009.06.002.
- 536 **Mugnier, MR, Stebbins, CE and Papavasiliou, FN** (2016) Masters of Disguise: Antigenic
537 Variation and the VSG Coat in *Trypanosoma brucei*. *PLoS Pathogens* **12**, 1–6. doi:
538 10.1371/journal.ppat.1005784.

- 539 **Openshaw, AEA, Race, PR, Monzó, HJ, Vázquez-Boland, J-A and Banfield, MJ** (2005)
540 Crystal structure of SmcL, a bacterial neutral sphingomyelinase C from *Listeria*.
541 *Journal of Biological Chemistry* **280**, 35011–7. doi: 10.1074/jbc.M506800200.
- 542 **Richmond, GS and Smith, TK** (2007a) A novel phospholipase from *Trypanosoma brucei*.
543 *Molecular Microbiology* **63**, 1078–1095. doi: 10.1111/j.1365-2958.2006.05582.x.A.
- 544 **Richmond, GS and Smith, TK** (2007b) The role and characterization of phospholipase A1
545 in mediating lysophosphatidylcholine synthesis in *Trypanosoma brucei*. *Biochemical*
546 *Journal* **405**, 319–29. doi: 10.1042/BJ20070193.
- 547 **Richmond, GS, Gibellini, F, Young, SA, Major, L, Denton, H, Lilley, A and Smith, TK**
548 (2010) Lipidomic analysis of bloodstream and procyclic form *Trypanosoma brucei*.
549 *Parasitology* **137**, 1357–92. doi: 10.1017/S0031182010000715.
- 550 **Serricchio, M and Bütikofer, P** (2011) *Trypanosoma brucei*: a model micro-organism to
551 study eukaryotic phospholipid biosynthesis. *FEBS journal* **278**, 1035–46. doi:
552 10.1111/j.1742-4658.2011.08012.x.
- 553 **Sevova, ES, Goren, MA, Schwartz, KJ, Hsu, F-F, Turk, J, Fox, BG and Bangs, JD**
554 (2010) Cell-free synthesis and functional characterization of sphingolipid synthases
555 from parasitic trypanosomatid protozoa. *Journal of Biological Chemistry* **285**, 20580–7.
556 doi: 10.1074/jbc.M110.127662.
- 557 **Shaw, APM, Cecchi, G, Wint, GRW, Mattioli, RC and Robinson, TP** (2014) Mapping the
558 economic benefits to livestock keepers from intervening against bovine trypanosomosis
559 in Eastern Africa. *Preventive Veterinary Medicine* **113**, 197–210. doi:
560 10.1016/j.prevetmed.2013.10.024.
- 561 **Smith, TK and Bütikofer, P** (2010) Lipid metabolism in *Trypanosoma brucei*. *Molecular*
562 *and Biochemical Parasitology* **172**, 66–79. doi: 10.1016/j.molbiopara.2010.04.001.
- 563

- 564 **Sutterwala, SS, Hsu, F-F, Sevova, ES, Schwartz, KJ, Zhang, K, Key, P, Turk, J,**
565 **Beverley, SM and Bangs, JD** (2008) Developmentally regulated sphingolipid synthesis
566 in African trypanosomes. *Molecular Microbiology* **70**, 281–96. doi: 10.1111/j.1365-
567 2958.2008.06393.x.
- 568 **Tidhar, R and Futerman, AH** (2013) The complexity of sphingolipid biosynthesis in the
569 endoplasmic reticulum. *Biochimica et Biophysica Acta* **1833**, 2511–8. doi:
570 10.1016/j.bbamcr.2013.04.010.
- 571 **Uemura, A, Watarai, S, Kushi, Y, Kasama, T, Ohnishi, Y and Kodama, H** (2006)
572 Analysis of neutral glycosphingolipids from *Trypanosoma brucei*. *Veterinary*
573 *Parasitology* **140**, 264–272. doi: 10.1016/j.vetpar.2006.04.028.
- 574 **Wirtz, E, Leal, S, Ochatt, C and Cross, GA** (1999) A tightly regulated inducible expression
575 system for conditional gene knock-outs and dominant-negative genetics in *Trypanosoma*
576 *brucei*. *Molecular and Biochemical Parasitology* **99**, 89–101.
- 577 **World Health Organization** (2017a) Trypanosomiasis, human African (sleeping sickness).
578 Retrieved from the World Health Organization website:
579 <http://www.who.int/mediacentre/factsheets/fs259/en/> (accessed 25 August 2017)
- 580 **World Health Organization** (2017b) *Integrating neglected tropical diseases into global*
581 *health and development: fourth WHO report on neglected tropical diseases*. Geneva,
582 Switzerland: World Health Organization.
- 583 **Xu, W, Xin, L, Soong, L and Zhang, K** (2011) Sphingolipid degradation by *Leishmania*
584 *major* is required for its resistance to acidic pH in the mammalian host. *Infection and*
585 *Immunity* **79**, 3377–87. doi: 10.1128/IAI.00037-11.
- 586 **Young, SA and Smith, TK** (2010) The essential neutral sphingomyelinase is involved in the
587 trafficking of the variant surface glycoprotein in the bloodstream form of *Trypanosoma*
588 *brucei*. *Molecular Microbiology* **76**, 1461–82. doi: 10.1111/j.1365-2958.2010.07151.x.

- 589 **Zhang, K, Pompey, JM, Hsu, F-F, Key, P, Bandhuvula, P, Saba, JD, Turk, J and**
 590 **Beverley, SM** (2007) Redirection of sphingolipid metabolism toward de novo synthesis
 591 of ethanolamine in *Leishmania*. *EMBO journal* **26**, 1094–104. doi:
 592 10.1038/sj.emboj.7601565.
- 593 **Zhang, O, Wilson, MC, Xu, W, Hsu, F-F, Turk, J, Kuhlmann, FM, Wang, Y, Soong, L,**
 594 **Key, P, Beverley, SM and Zhang, K** (2009) Degradation of host sphingomyelin is
 595 essential for *Leishmania* virulence. *PLoS pathogens* **5**, e1000692. doi:
 596 10.1371/journal.ppat.1000692.
- 597 **Zhang, O, Xu, W, Balakrishna Pillai, A and Zhang, K** (2012) Developmentally regulated
 598 sphingolipid degradation in *Leishmania major*. *PloS one* **7**, e31059. doi:
 599 10.1371/journal.pone.0031059.

600

601 **FIGURE LEGENDS**

602 **Fig. 1: *Trypanosoma brucei* sphingolipid metabolism.** A) The currently proposed pathway for *T. brucei*
 603 *de novo* sphingolipid biosynthesis is shown. SPT-serine-palmitoyltransferase (Q580D0);
 604 3-KSR – 3-ketosphinganine reductase (Q38BJ6); CerS – ceramide synthase (Q57V92, Q583F9);
 605 DES – dihydroceramide desaturase (Q583N4); TbSLSs 1-4 – *T. brucei* sphingolipid synthases 1-4 (Q38E53;
 606 Q38E54; Q38E55; Q38E56). Biosynthesis of ceramide (36:1) has been used here as an example.
 607 B) A simplified overview of eukaryotic sphingolipid degradation is provided (omitting glycosphingolipid
 608 catabolic pathways). A representative sphingolipid species (sphingomyelin (36:1)) is degraded in a step-wise
 609 process involving sphingomyelinases (SMases) and ceramidases (CDases). Lipid headgroups, such as choline
 610 phosphate, and sphingosine can be recycled to participate in *de novo* biosynthesis via the salvage pathway
 611 (green dashed arrows). Products ceramide and sphingosine can also be phosphorylated to produce signalling
 612 molecules ceramide-1-phosphate and sphingosine-1-phosphate respectively. ATP – adenosine triphosphate;
 613 ADP – adenosine diphosphate; CERK – ceramide kinase; SphK – sphingosine kinase.

614 **Fig. 2: ESI-MS/MS analysis of sphingomyelin substrate reactions.** Spectra are ESI-MS/MS precursor ion
 615 scans to detect choline-containing lipids (precursors of m/z 184) in positive ion mode.
 616 A) GST-TbnSMase-enriched bacterial membranes plus SM substrate. B) heat-inactivated GST-TbnSMase
 617 enriched bacterial membranes plus SM substrate. (†) Highlights the dimyristoyl-PC (28:0) standard
 618 (500 pmoles). C) Peak intensities (cps), normalised against the intensity of the dimyristoyl-PC (28:0) standard,

619 for each significant sphingomyelin (SM) substrate lipid species are depicted. Values are mean intensities for
620 triplicate reactions ($n = 3$). Error bars represent the standard error of each mean (\pm).

621 **Fig. 3: GST-TbnSMase catabolism of sphingomyelin yields ceramide and choline phosphate.** Spectra are
622 ESI-MS/MS survey scans in negative ion mode. A) GST-TbnSMase-enriched bacterial membranes plus SM
623 substrate. B) heat-inactivated TbnSMase-enriched bacterial membranes plus SM substrate. Annotated ceramides
624 have formed chloride adducts $[M + Cl]^-$. (*) Highlights previously identified significant contaminants of
625 negative ion mode surveys thought to be associated with the detergent. C) Aqueous fractions of sphingomyelin
626 substrate reactions were used as substrates for the Amplex® UltraRed assay system, plus (+) or minus (-) the
627 coupling-enzyme alkaline phosphatase (AlkPhos). Change in fluorescence (millirelative-fluorescence units per
628 minute (mrfu min^{-1})) was monitored spectrophotometrically. Values represent average rate of fluorescence
629 change for aqueous fractions derived from triplicate reactions ($n = 3$). Error bars represent the standard error of
630 each mean (\pm).

631 **Fig. 4: ESI-MS/MS analysis of ethanolamine-phosphoceramide substrate reactions.** Spectra are
632 ESI-MS/MS survey scans in negative ion mode. A) EPC only (minus Triton X-100 detergent).
633 B) GST-TbnSMase-enriched bacterial membranes plus EPC substrate. Annotated ceramides have formed
634 chloride adducts $[M + Cl]^-$. C) heat-inactivated GST-TbnSMase-enriched bacterial membranes plus EPC
635 substrate. D) EPC/ Triton X-100 detergent mixed micelle substrate only. (*) Highlights previously identified
636 significant contaminants of negative ion mode surveys thought to be associated with the detergent.

637 **Fig. 5: ESI-MS/MS analysis of *T. brucei* procyclic-extract (inositol-phosphoceramide) substrate reactions.**
638 A) ESI-MS/MS precursor ion scan of the procyclic lipid extract (IPC substrate) to detect inositol-containing
639 lipids (precursors of m/z 241), in negative ion mode. The extract contains dihydroxylated ceramides, as well as
640 trihydroxylated ceramides, the later denoted as 't'. B) ESI-MS/MS negative ion mode survey scans were used to
641 detect ceramides in GST-TbnSMase and C) heat-inactivated GST-TbnSMase-enriched bacterial membranes
642 plus IPC substrate reactions. Annotated ceramides have formed chloride adducts $[M + Cl]^-$.

643 **Fig. 6: GST-TbnSMase catabolism of ceramide-1-phosphate yields ceramide.** Spectra are ESI-MS/MS
644 survey scans in negative ion mode. A) GST-TbnSMase-enriched bacterial membranes plus
645 ceramide-1-phosphate (C-1-P) substrate. B) Non-TbnSMase-expressing bacterial membranes plus
646 ceramide-1-phosphate substrate. The annotated ceramide (Cer) product species has formed a
647 chloride adduct $[M + Cl]^-$.

648 **Fig. 7: ESI-MS/MS analysis of lyso-PC substrate reactions.** Spectra are ESI-MS/MS precursor ion scans to
649 detect choline-containing lipids (precursors of m/z 184) in positive ion mode. A) GST-TbnSMase-enriched
650 bacterial membranes with lyso-PC substrate. B) non-TbnSMase-expressing bacterial membranes with lyso-PC
651 substrate. (†) Highlights the didecanoyl-PC (20:0) standard (500 pmoles). (*) Highlights previously identified
652 significant contaminants of positive ion mode scans thought to be associated with the detergent.

SUPPLEMENTARY MATERIAL

Full title: Investigating the Substrate Specificity of the Neutral Sphingomyelinase
from *Trypanosoma brucei*

Emily A. Dickie¹, Simon A. Young and Terry K. Smith

Biomedical Sciences Research Complex, Schools of Biology and Chemistry, University of St
Andrews, Fife, KY169ST, UK

Running title: *T. brucei* neutral sphingomyelinase substrate specificity

Correspondence should be addressed to Terry K. Smith. Address: Biomedical Sciences
Research Complex, Schools of Biology and Chemistry, University of St Andrews, Fife,
KY169ST, UK. Telephone: +44(0)1334 463412. Email: tks1@st-andrews.ac.uk

¹ Current address: Wellcome Trust Centre for Molecular Parasitology, Institute of Infection,
Immunity and Inflammation, College of Medical, Veterinary and Life Sciences, University of
Glasgow, Glasgow, G12 8TA, UK

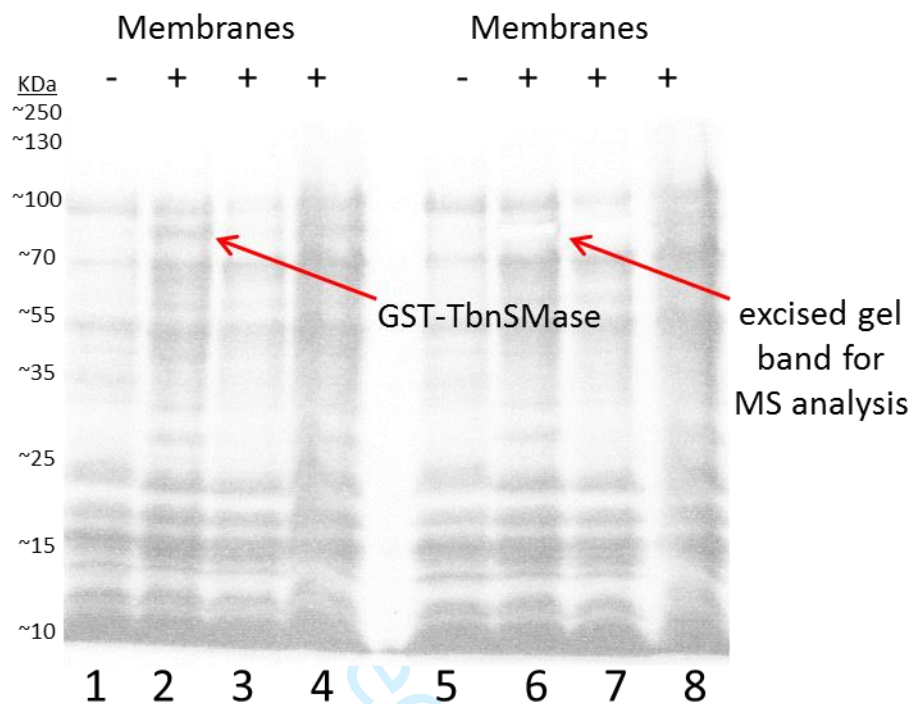


Fig. S1: Presence of GST-TbnSMase in bacterial membranes was confirmed by mass spectrometry analysis. pLysSGold *E. coli* membrane fractions were separated via SDS-PAGE and stained with Coomassie. Fractions were run in duplicate (lanes 1-4 and again, in lanes 5-8). '-' indicates the non-TbnSMase-expressing control bacterial membranes. '+' signifies membrane fractions were derived from *E. coli* expressing GST-TbnSMase. The band thought to correspond to GST-TbnSMase (annotated, lane 2) was excised (annotated, lane 6) and submitted for mass spectrometry analysis, which confirmed its identity as GST-TbnSMase.

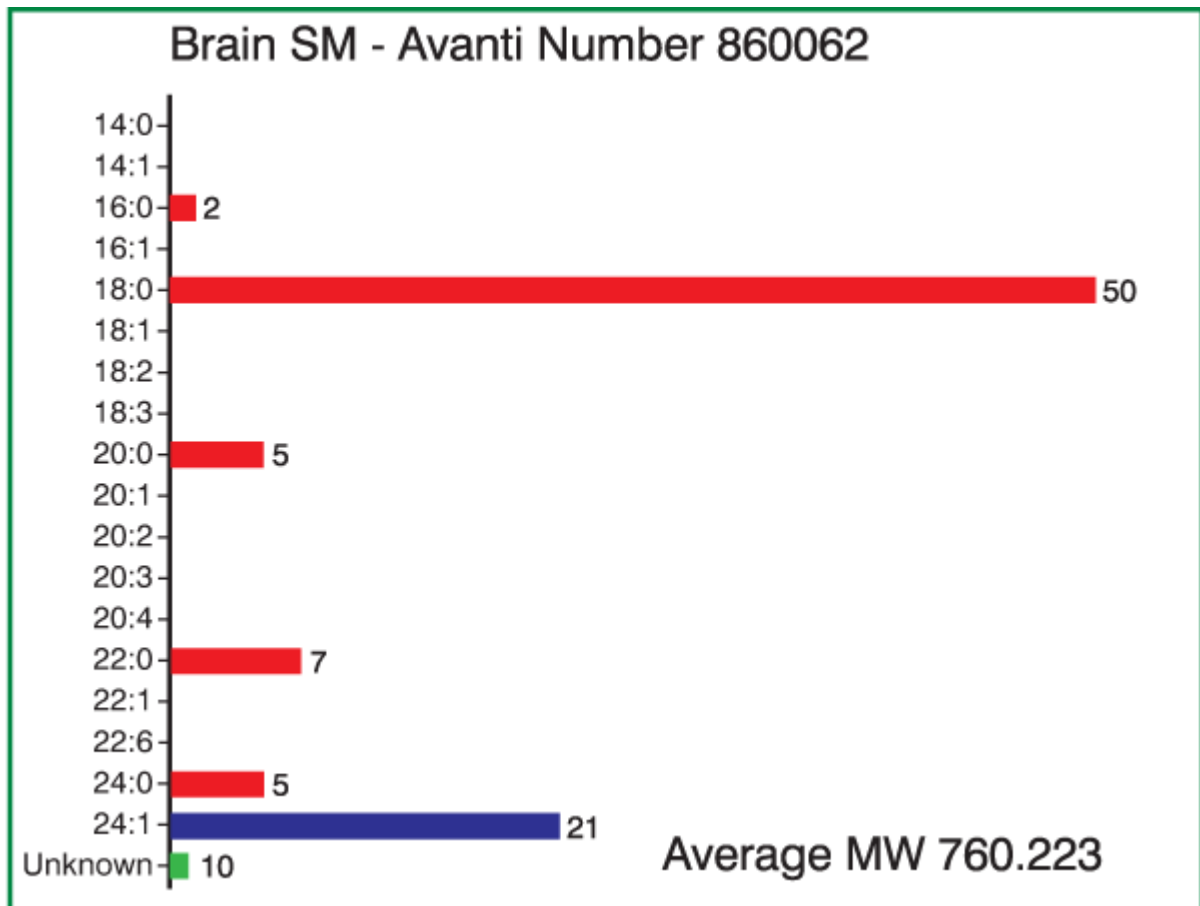


Fig S2: Avanti fatty acid analysis of brain SM product 860062. This product (<https://avantilipids.com/product/860062>) was used as an SM substrate for GST-TbnSMase (see **Fig. 2** and **Fig. S3**). Average fatty acid distribution for SM (d18:1/y) lipid species within the product are shown.

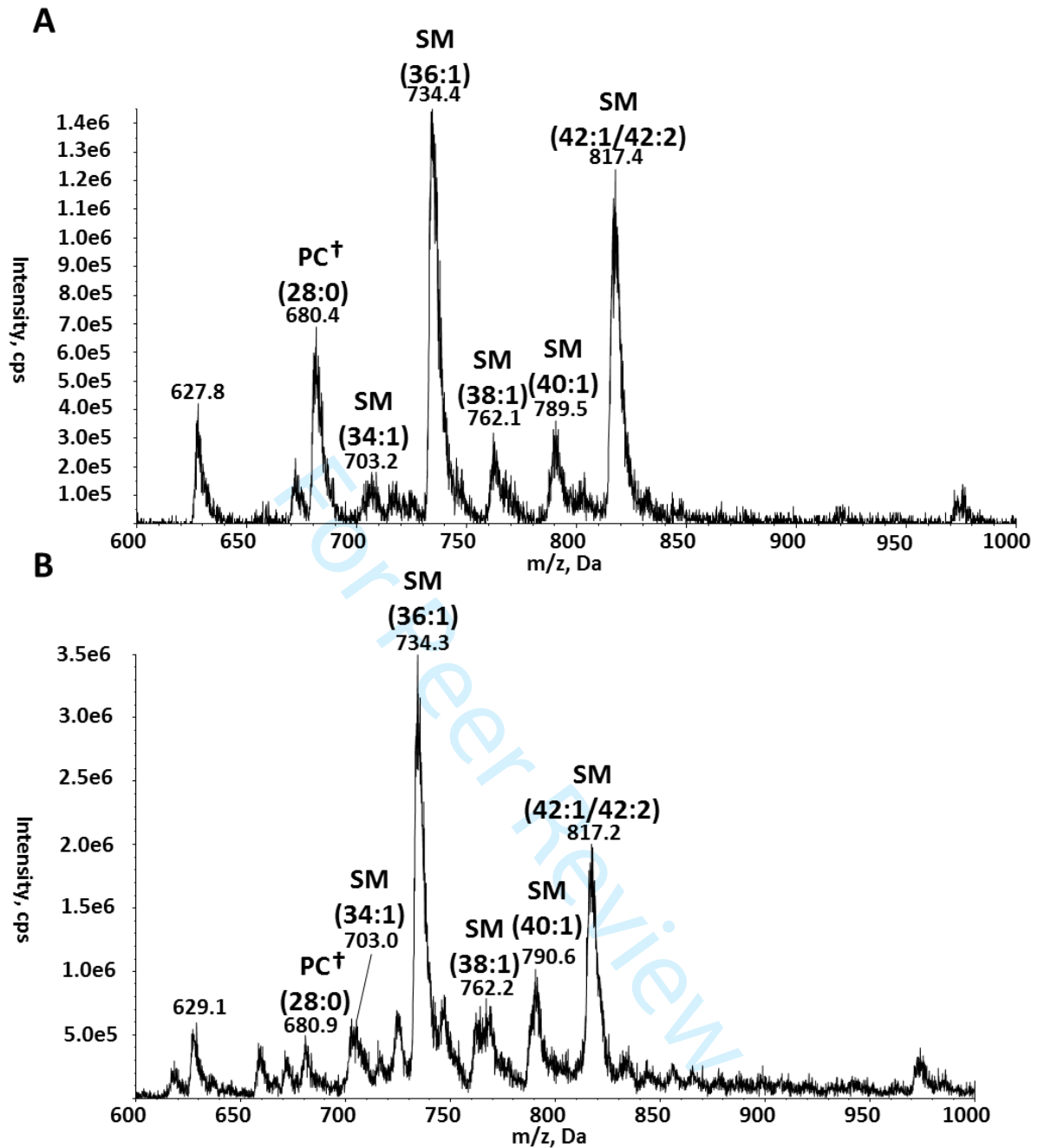


Fig. S3: Additional supporting spectra for GST-TbnSMase catabolism of sphingomyelin. Spectra are ESI-MS/MS precursor ion scans to detect choline-containing lipids (precursors of m/z 184) in positive ion mode. A) SM/Triton X-100 mixed micelle substrate only. B) Non-TbnSMase-expressing bacterial membranes plus SM substrate. (†) Highlights the dimyristoyl-PC (28:0) standard (500 pmoles).

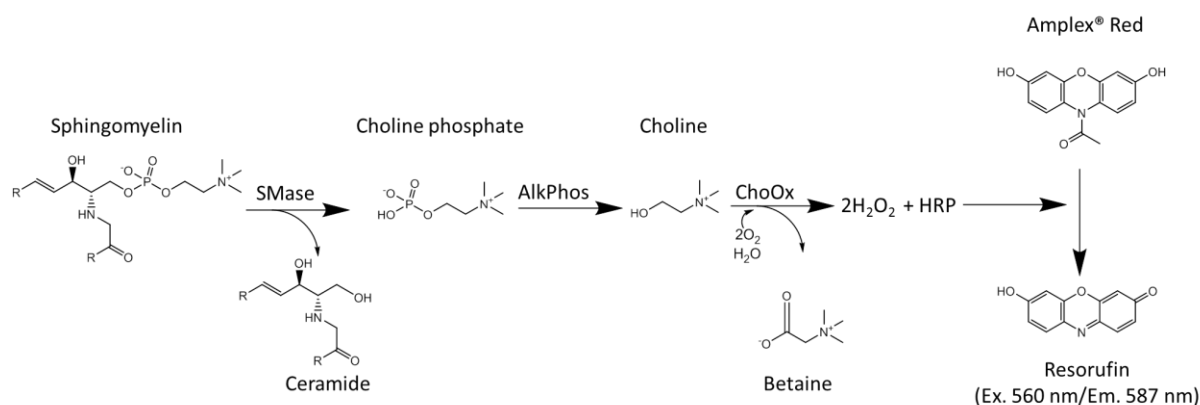


Fig. S4: Amplex® Red assay system. Sphingomyelinase (SMase) activity results in sphingomyelin substrate catabolism, producing ceramide and choline-phosphate (ChoP). ChoP is then hydrolysed by the assay coupling enzyme alkaline phosphatase (AlkPhos), forming choline (Cho). Choline oxidase (ChoOx) oxidises choline to yield betaine and hydrogen peroxide (H₂O₂). As the ChoOx used in the assay is isolated from *Alcaligenes sp.*, Cho is fully oxidised to betaine, via a betaine-aldehyde intermediate (not shown), and 2 moles of hydrogen peroxide (H₂O₂) are produced for every mole of Cho. The H₂O₂ is the oxidising agent for horseradish peroxidase (HRP) that catalyses the conversion of Amplex® Red to red-fluorescent resorufin. The rate of this conversion can be monitored spectrophotometrically (Ex. 560 nm, Em. 587 nm). For the work described here, Amplex® UltraRed, an optimised version of Amplex® Red, was used. However, no chemical structure or formula is available for Amplex® UltraRed and its red-fluorescent conversion product.

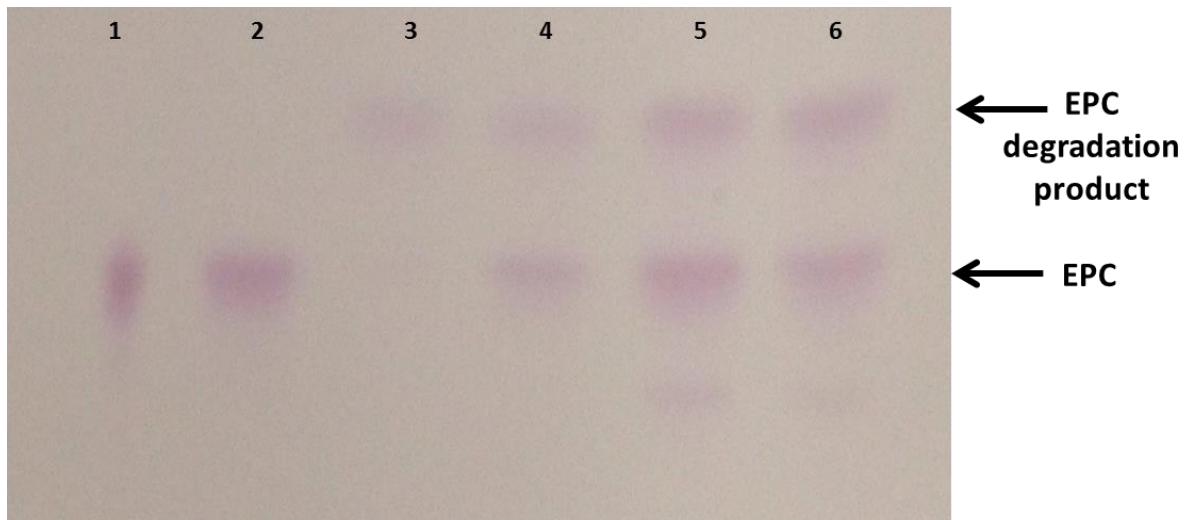


Fig. S5: HPTLC analysis of ethanolamine-phosphoceramide substrate reactions.

1) EPC stock solution (no Triton X-100 detergent); 2) EPC/Triton X-100 detergent mixed micelle substrate in reaction buffer; 3) GST-TbnSMase-enriched bacterial membranes plus EPC substrate; 4) non-TbnSMase-expressing bacterial membranes plus EPC substrate; 5) heat-inactivated GST-TbnSMase-enriched bacterial membranes plus EPC substrate; 6) heat-inactivated non-TbnSMase-expressing bacterial membranes plus EPC substrate.

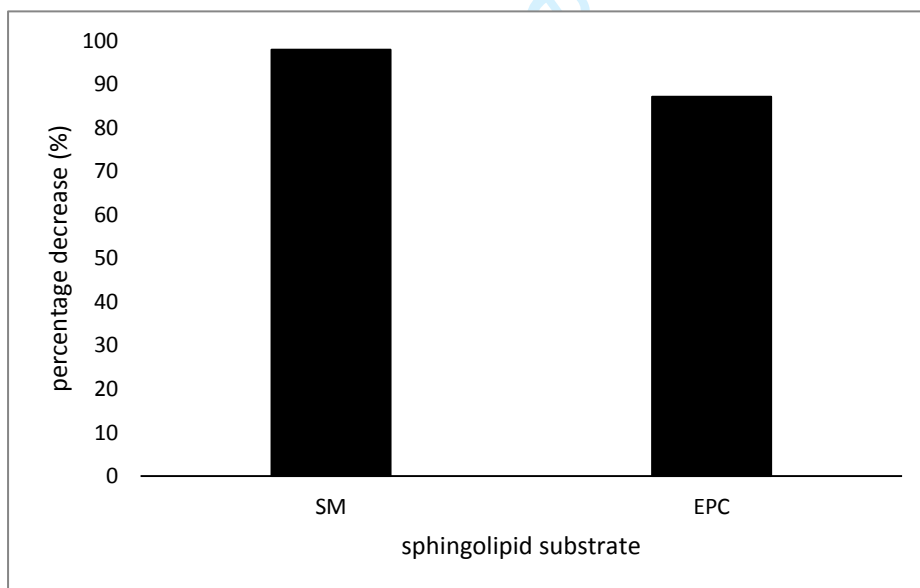


Fig. S6: Spingomyelin and ethanolamine-phosphoceramide substrate competition assay. A substrate mixture, containing equimolar concentrations (25 nmoles) of spingomyelin and ethanolamine-phosphoceramide, was incubated with GST-TbnSMase. The percentage decreases (%) in the level of each substrate, relative to a TbnSMase negative control, are shown.

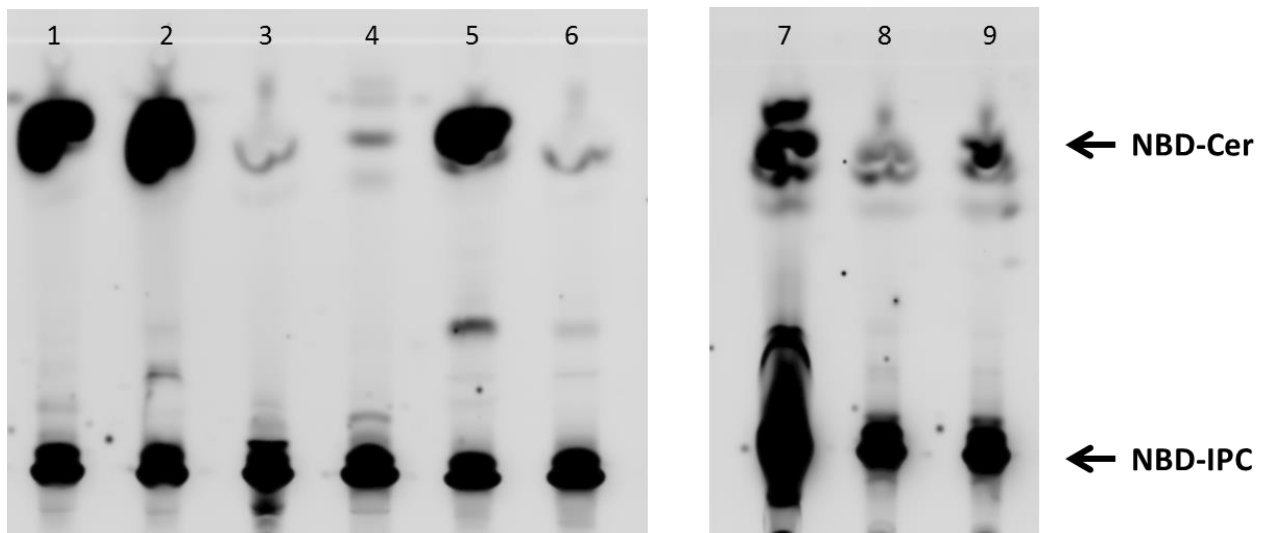


Fig. S7: HPTLC analysis of NBD-IPC substrate reactions. 1) bloodstream form *T. brucei* lysate with NBD-IPC substrate; 2) stumpy form *T. brucei* lysate with NBD-IPC substrate; 3) procyclic form *T. brucei* lysate with NBD-IPC substrate (stored prior to use); 4) NBD-IPC substrate only; 5) GST-TbnSMase-expressing *E. coli* lysate with NBD-IPC substrate; 6) non-GST-TbnSMase-expressing *E. coli* lysate with NBD-IPC substrate; 7) procyclic form *T. brucei* lysate with NBD-IPC substrate (freshly prepared); 8) promastigote form *L. major* lysate with NBD-IPC substrate; 9) epimastigote form *T. cruzi* lysate with NBD-IPC substrate.

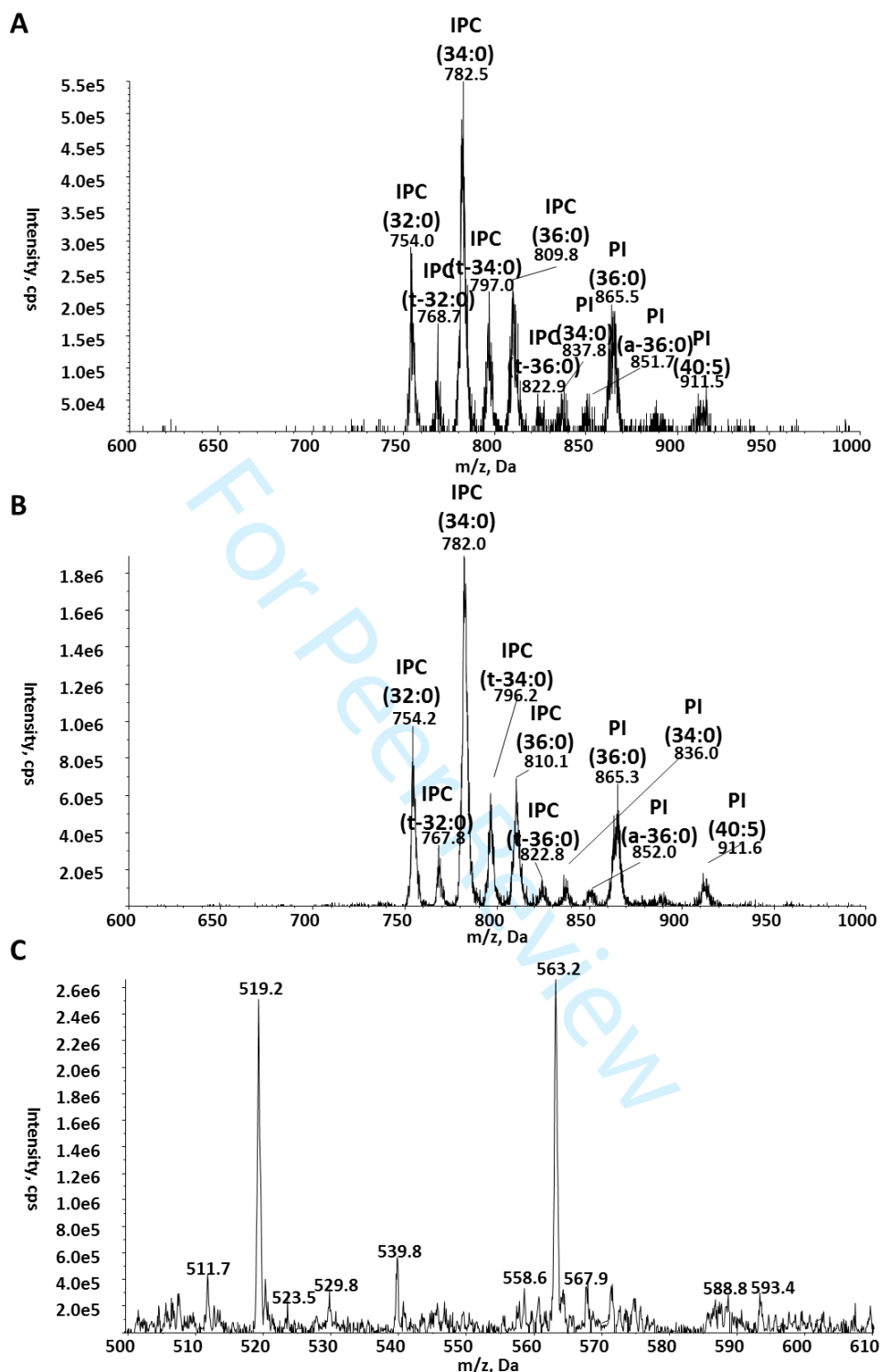
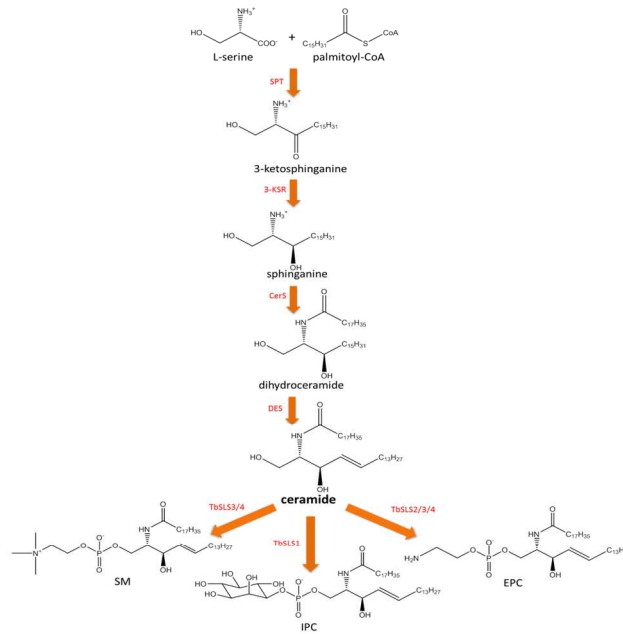


Fig. S8: Additional supporting spectra for *T. brucei* procyclic-extract (inositol-phosphoceramide) reactions. ESI-MS/MS precursor ion scans to detect inositol-containing lipids (precursors of m/z 241) in negative ion mode. A) GST-TbnSMase-enriched bacterial membranes plus procyclic extract (IPC) substrate. B) heat-inactivated GST-TbnSMase-enriched bacterial membranes plus IPC substrate. The substrate contains dihydroxylated ceramides, as well as trihydroxylated ceramides, the later denoted as 't-'. C) ESI-MS/MS survey scan, in negative ion mode, of the IPC/Triton X-100 detergent mixed micelle substrate only.

A



B

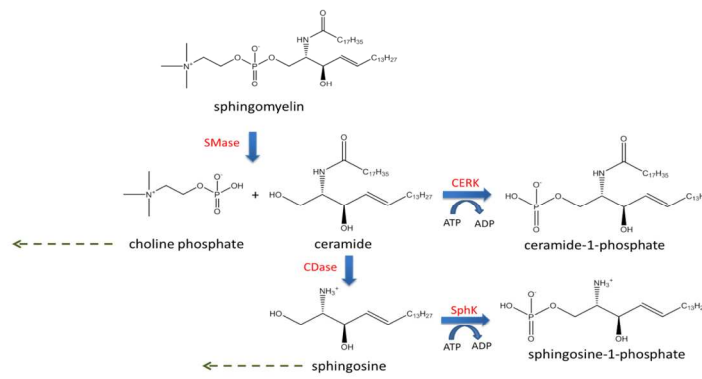


FIG 1

190x275mm (192 x 192 DPI)

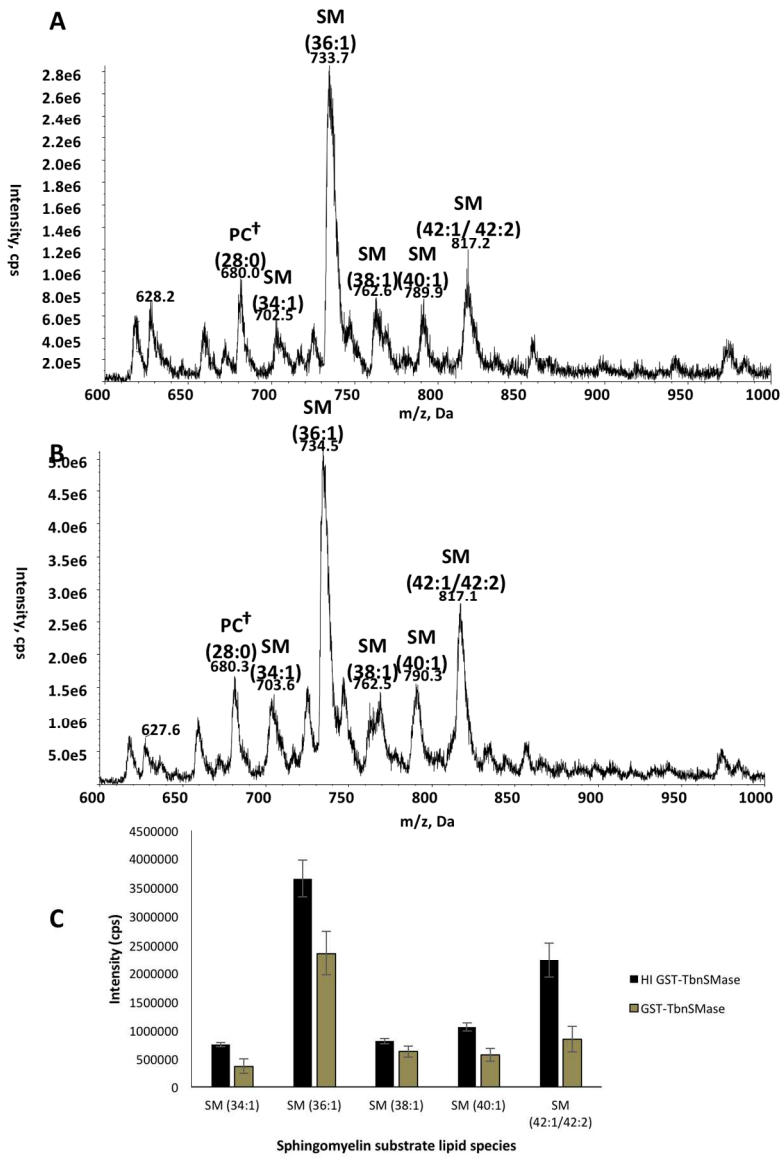


FIG 2

190x275mm (192 x 192 DPI)

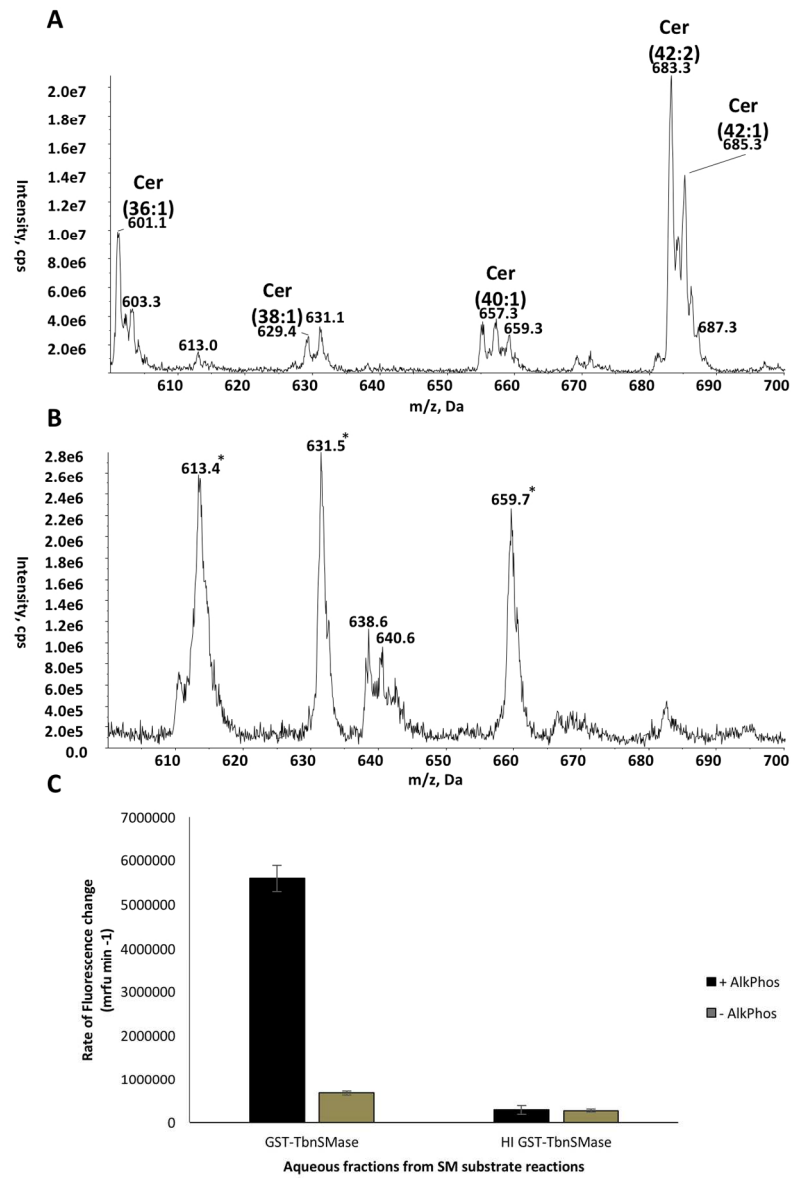


FIG 3

190x275mm (192 x 192 DPI)

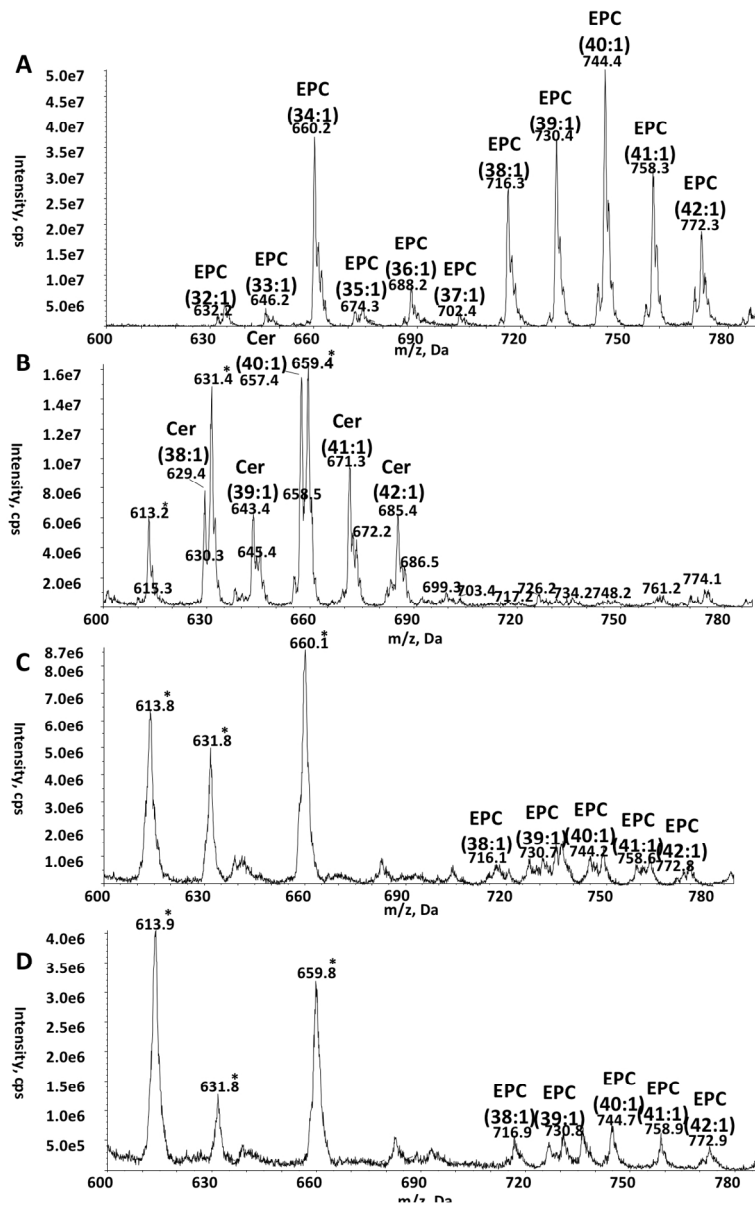


FIG 4

190x275mm (192 x 192 DPI)

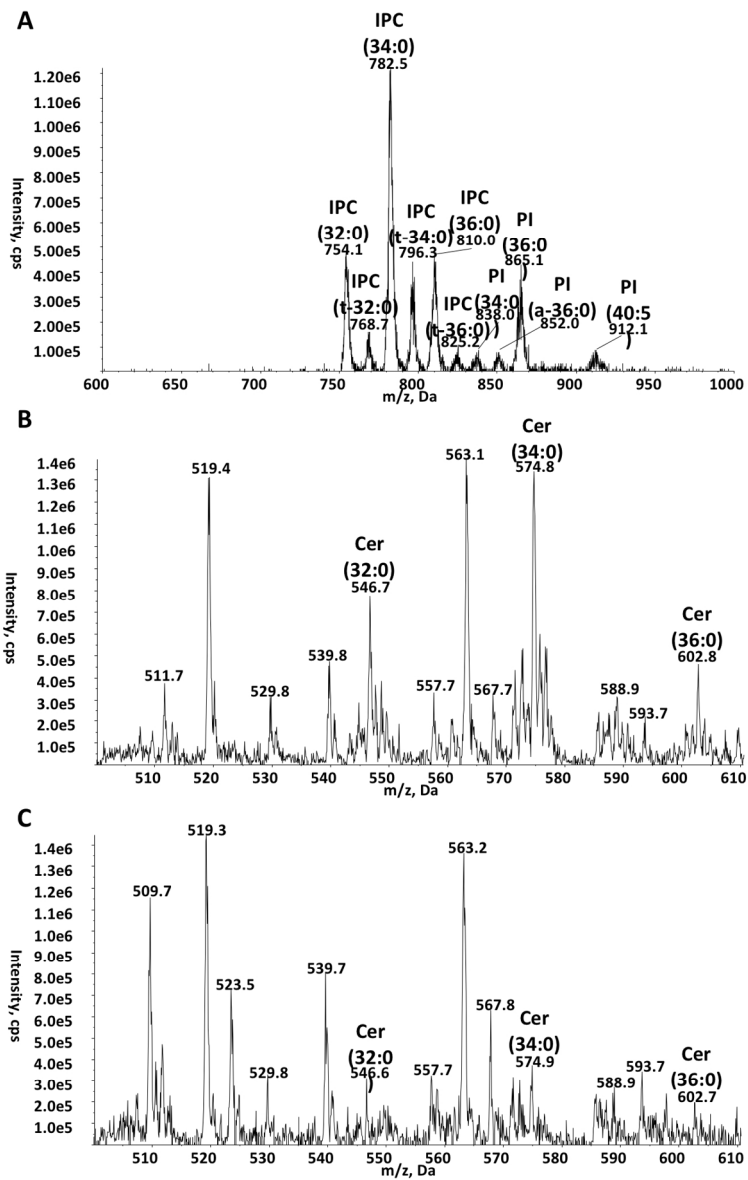


FIG 5

190x275mm (192 x 192 DPI)

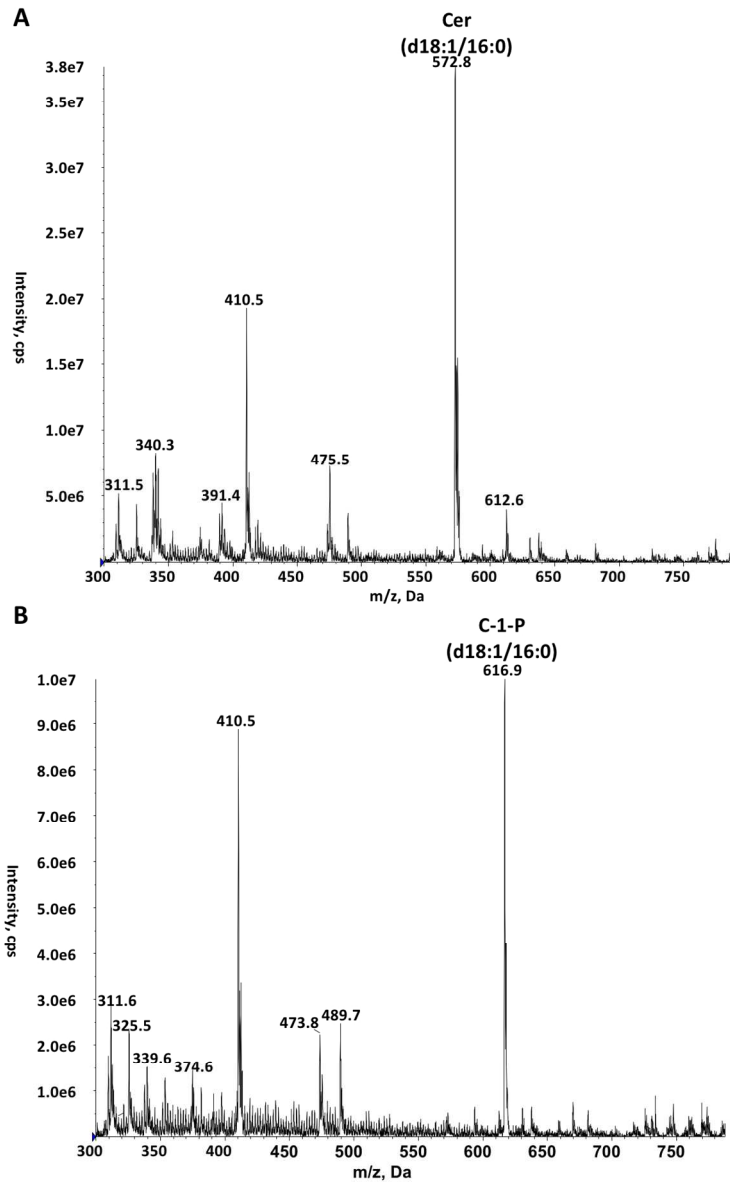


fig 6

190x275mm (192 x 192 DPI)

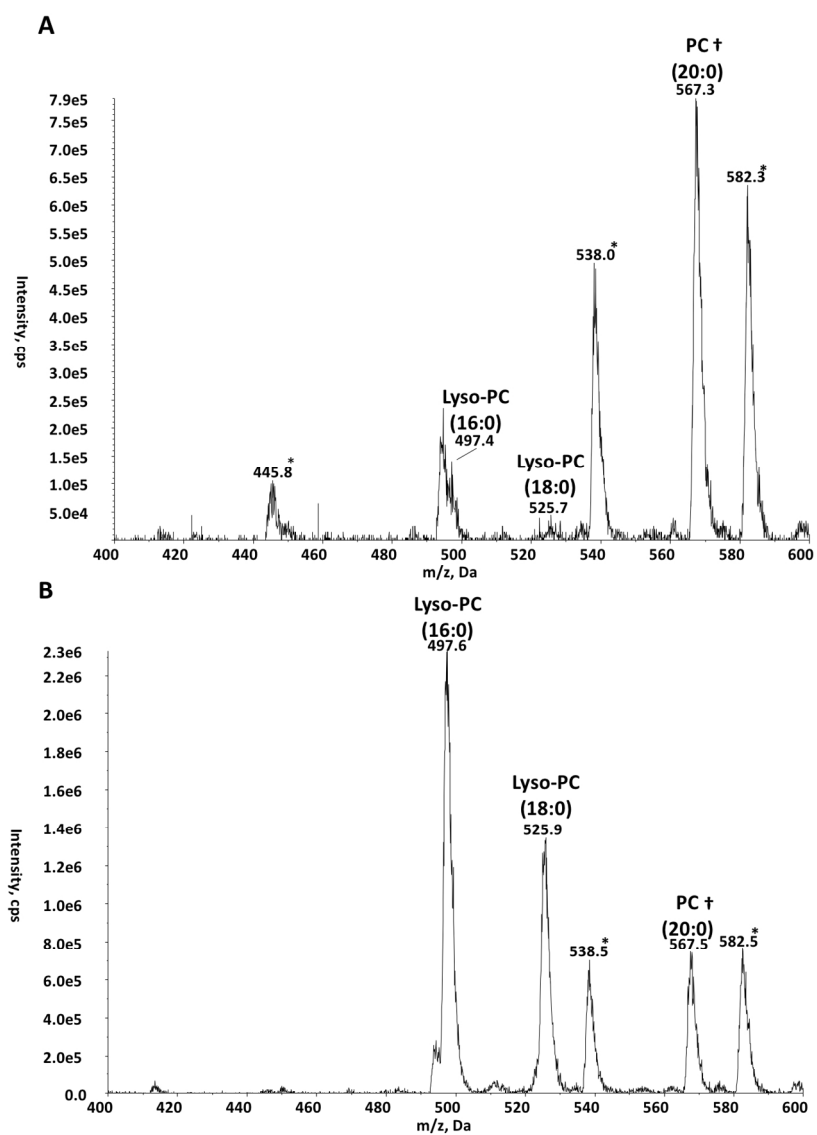


fig 7

190x275mm (192 x 192 DPI)